Meteorologische Zeitschrift, Vol. **17**, No. 4, 383-394 (August 2008)

Article

Towards climate simulations at cloud-resolving scales

CATHY HOHENEGGER*, PETER BROCKHAUS and CHRISTOPH SCHÄR

Institute for Atmospheric and Climate Science, ETH Zürich, Switzerland

(Manuscript received November 13, 2007; in revised form February 16, 2008; accepted May 5, 2008)

Abstract

This study explores the potential added-value of applying cloud-resolving resolution to climate simulations. A month-long (July 2006) integration is performed with the CCLM on a convection-resolving grid of 2.2-km (0.02°) mesh size spanning the whole Alpine region. The initial and lateral boundary conditions stem from a coarser-resolution 25-km (0.22°) CCLM integration. Comparison to observations indicates that the cloud-resolving simulation is able to capture the overall precipitation distribution and evolution. With respect to its driving lower-resolution integration, the cloud-resolving resolution yields a more accurate spatial localization of the precipitation maxima, reduces the cold bias, and especially reproduces a better timing of the convective diurnal cycle. The explicit resolution delays the onset of convective precipitation by about 2 h, shifts the time of peak precipitation by a similar period, and slows down the decay of convective activity in the afternoon. In return, the integration shows a tendency to underestimate the afternoon convective rainfalls, particularly under weak synoptic and/or orographic forcing. This latter effect might be improved by modifying the treatment of subgrid-scale clouds in the model.

Zusammenfassung

Die vorliegende Studie untersucht den potentiellen Mehrwert von wolkenauflösenden Klimasimulationen. Es wird eine einmonatige Simulation (Juli 2006) mit dem CCLM-Modell vorgestellt, die den gesamten Alpenraum mit einem 2.2-km-Gitter (0.02°) abdeckt. Die Randdaten stammen von einem 25-km-Lauf (0.22°) mit dem selben Modell. Der Vergleich mit Beobachtungen zeigt, dass die wolkenauflösende Simulation die räumliche und zeitliche Niederschlagsverteilung wiedergeben kann. Verglichen mit der antreibenden Simulation mit ihrer gröberen Auflösung verbessert der wolkenauflösende Lauf die räumliche Verteilung der Niederschlags-Maxima, reduziert die Unterschätzung der Temperatur und verbessert insbesondere den Zeitpunkt des konvektiven Niederschlags. Die explizite Auflösung verzögert den Niederschlagsbeginn und die Zeit des Niederschlagsmaximums um 2 h und verlangsamt den Zerfall der konvektiven Aktivität am Nachmittag. Allerdings unterschätzt der Lauf den konvektiven Niederschlag am Nachmittag, und dies ganz besonders bei schwachem synoptischen und/oder orographischen Antrieb. Dieser Effekt könnte jedoch mit einer angepassten Behandlung von kleinen, nicht-aufgelösten Wolken reduziert werden.

1 Introduction

Regional climate models have become over the past years highly sophisticated numerical constructs embodying a detailed description of physical processes and addressing multi-decadal time frames on grids of typically 15–50 km mesh size (see CHRISTENSEN et al., 2007b; GIORGI, 2006; MCGREGOR, 1997). Numerous studies have been devoted to their development, tuning, intercomparison, and improvement (e.g., JACOB et al., 2007; CHRISTENSEN et al., 2007b; VIDALE et al., 2003; FREI et al., 2003; HAGEMANN et al., 2004; GIORGI and MEARNS, 1999). They have enabled RCMs to become useful tools for the simulation of present-day and future climates (see especially RANDALL et al., 2007; CHRISTENSEN et al., 2007a) and for process studies (e.g., WANG et al., 2004; PIELKE et al., 2007; FISCHER et al., 2007).

However, despite continuous progress, RCMs are imperfect by nature and bear considerable limitations. One uncertain issue concerns the projection of summertime precipitation changes over Europe, which strongly relies on the chosen model formulation (DEQUE et al., 2007) and interferes with seasonal variability changes (SCHÄR et al., 2004; VIDALE et al., 2007). Difficulties arise due to the weaker synoptic-scale forcing, the predominance of moist convection, and the key role played by land-surface processes (e.g., SENEVIRATNE et al., 2006). Convective parameterizations are a known source of major uncertainties and errors in the simulation of present-day and future climates (see e.g., MOLINARI and DUDEK, 1992; DAI et al., 1999; BROCKHAUS et al., 2008). Symptomatic to many RCMs is the use of convective parameterizations which have been primarily developed to mimic convection over the Tropics with a relatively coarse (50–100-km) mesh size.

In order to improve some of the aspects of the simulated summer climate and given nowadays computer capabilities, one of the natural pathway leads towards reducing the RCM grid spacing down to some few kilometers (LEUNG et al., 2006, 2003; WANG et al., 2004). The application of such cloud-resolving models has in principle two main advantages. First, they allow a better representation of topography and surface fields. Second,

*Corresponding author: Cathy Hohenegger, Institute for Atmospheric and Climate Science, ETH Zürich, Universitätstr. 16, 8092 Zürich, Switzerland, e-mail: cathy.hohenegger@env.ethz.ch

0941-2948/2008/0303 $ 5.40

DOI 10.1127/0941-2948/2008/0303

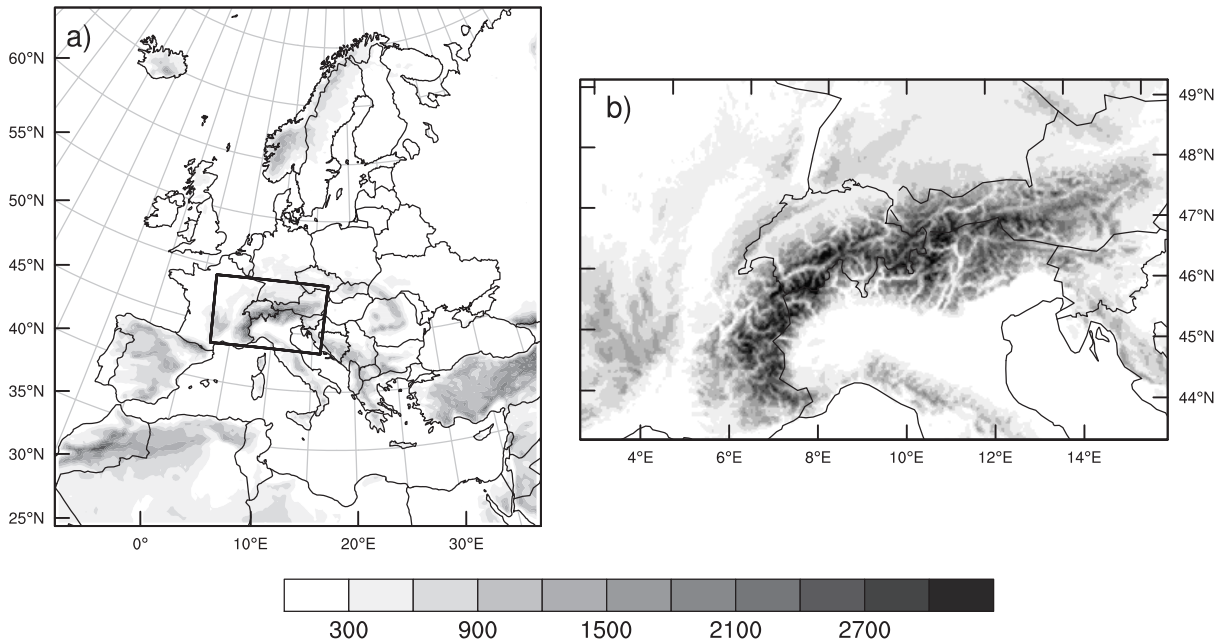

Figure 1: Integration domain and topography (m) of (a) the driving 25-km and (b) the cloud-resolving 2.2-km CCLM simulation.

deep convection can be explicitly resolved in place of uncertain parameterizations. On the other hand, cloud-resolving integrations also pose several challenges in terms of required computational resources, dynamical, and physical packages (see e.g., WANG et al., 2004; STEPPELER et al., 2003b). In particular, they impose the relaxation of the hydrostatic approximation which is still widely employed for climate studies.

The use of cloud-resolving numerical models is now common practice for numerical weather prediction (NWP), both operationally and for research purposes (see, e.g., MASS et al., 2002; COLLE et al., 2005; JANKOV et al., 2005; RICHARD et al., 2007; HOHENEGGER and SCHÄR, 2007), but is largely uncharted territory on longer time scales. From NWP experimentations (see especially MASS et al., 2002), it is generally accepted that cloud-resolving simulations yield a more realistic precipitation pattern, particularly in cases of moist convection and/or over mountainous regions. However, the gain is often not significant in terms of statistical skill scores. From a climatological point of view, GRELL et al. (2000) conducted a 1-km integration over the Loisach valley and parts of the Wetterstein and Karwendel massifs in Germany (46x46 grid points) for a 14-month period. They found significant differences between lower- and higher-resolution simulations. MIURA et al. (2007) performed a 7-d global integration with a 3.5-km grid spacing and concluded that their simulation was able to reproduce the development of typhoons and the organization of convective systems. Instead of integrating a full climate model at cloud-resolving scales, several studies have employed cloud-resolving parameterizations embedded at each cell of a global lower-resolution grid (so-called superparameterizations, see, e.g., KHAIROUTDINOV and RANDALL (2001); GRABOWSKI (2001); RANDALL et al. (2003); ARAKAWA (2004); WYANT et al. (2006)). Other studies have driven their cloud-resolving model by external forcings (e.g., BLOSSEY et al., 2007; KHAIROUTDINOV and RANDALL, 2003).

Here we present a pilot study devoted to the use of cloud-resolving (2.2-km) limited-area integrations on climatic time scales. We primarily seek to assess the suitability of cloud-resolving resolution for climate applications by comparing the performance of a month-long cloud-resolving integration to observations and to its driving lower-resolution simulation. As our model utilizes a horizontal resolution characteristic to weather forecasts but an integration period nearer to climatic time scales, our study in a way bridges the gap between weather and climate applications.

To attain our goals, we will take advantage of the nonhydrostatic limited-area model of the consortium for small-scale modeling (COSMO), which can be both applied for cloud-resolving NWP (DOMS and FÖRSTNER, 2004) and climate studies (see this issue). The model is integrated on a convection-resolving grid of 0.02° (2.2-km) mesh size that covers the Alpine region.

The simulation is carried out for one full month, July 2006. July 2006 was characterized by a flat pressure distribution, extremely hot temperatures, and a high potential for convective development. In France for instance (see METEOFRANCE, 2006), monthly mean temperatures exceeded the 30-y mean by 4° to 5°C. This places July 2006 at the second place after July 2003 of the warmest Julies since 1950. Over many parts of Switzer-

land, July 2006 was even warmer than July 2003 and many stations wrote record values. Even if we only restrict us to the simulation of July 2006, the high likelihood for convective development makes this month a particularly hard and suitable test to assess the performance of any model.

The outline is as follows. Section 2 describes our experimental set-up and the observational data sets used for validation purposes. The comparison of simulations and observations follows in section 3 in terms of precipitation, temperature, relative humidity, and radiation. The results are discussed in section 4 and concluded in section 5.

2 Method

2.1 Model

Our simulations are integrated with the CCLM (COSMO-CLM; COSMO model in CLimate Mode) version 4.0 as in JAEGER et al. (2008). This is a preliminary version of the official CCLM 4.0 release and in fact corresponds to the version 3.22 of the COSMO model. The COSMO model is a nonhydrostatic limited-area model developed by the German Weather Service (STEPPELER et al., 2003a) and subsequently adapted for climate studies (see this special issue). Its nonhydrostatic formulation and the recent updates of its dynamical and physical packages also allow its application on cloud-resolving scales (DOMS and FÖRSTNER, 2004). Today, it is used on a wide range of spatial (∼2 to 50 km grid spacing) and temporal (from days to decades) scales. For our study, the following dynamical and physical packages are utilized (see WILL et al. (submitted) for more details on the dynamics and physics of the model): the Runge-Kutta time-integration scheme (see FÖRSTNER and DOMS, 2004), the RITTER and GELEYN (1992) radiative transfer scheme, the multi-layer soil model (see HELMERT et al., submitted), turbulent kinetic energy considerations for the computation of the vertical fluxes of momentum and heat (see RASCHENDORFER, 2001), and the three-categories (ice, snow, graupel) ice scheme with prognostic treatment of the hydrometeors (see REINHARDT and SEIFERT, 2006). Most importantly, no convective parameterization is used.

We integrate the CCLM on a convection-resolving grid of 0.02° (2.2-km) over a domain covering the Alpine region (see Fig. 1). Our domain contains 501 by 301 grid points in the horizontal, 45 vertical levels, and 10 soil layers. The simulation, referred to as CCLM_2, starts 1 July 2006 and is integrated till 31 July 2006 with a time step of 40 s. All initial and lateral boundary conditions stem from a 0.22° (25-km) CCLM simulation. The latter integration, called CCLM_25, uses a 193 by 201 grid spanning the whole European continent, 32 vertical levels, 10 soil layers, and a 120-s time step. The initial and lateral boundary conditions are provided by the ECMWF operational analysis except for the initial soil moisture. The latter is taken from the corresponding field of a 25-km simulation which has been integrated over the whole 1958–2006 period. This ensures that the initial soil moisture is approximately within the equilibrium of the CCLM. Note that for CCLM_2, the initial soil moisture is directly taken from the initial soil moisture content of the CCLM_25 integration.

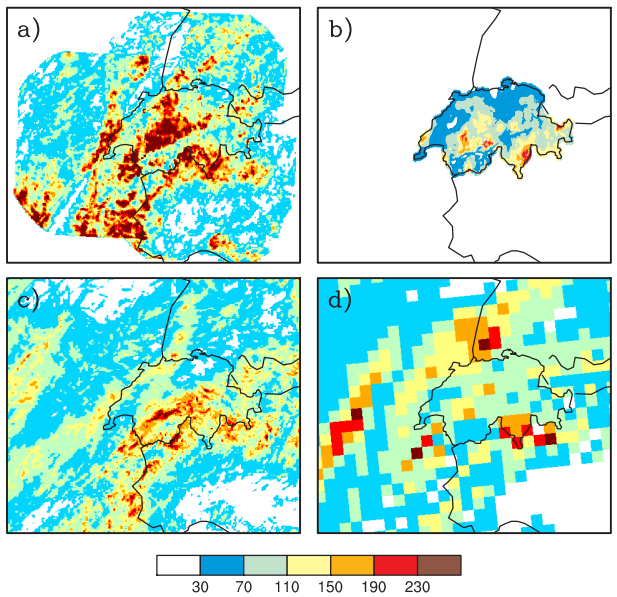

Figure 2: Maps of accumulated precipitation (mm; from 0600 UTC 1 July 2006 to 0600 UTC 31 July 2006) obtained in (a) RAD, (b) GAUGE, (c) CCLM_2, and (d) CCLM_25. Note that RAD and GAUGE only cover parts of the computational domain.

In opposition to CCLM_2, CCLM_25 employs Leapfrog dynamics. For grid-scale precipitation, graupel is not treated as a separate category. Also, deep convection must be parameterized at 25-km mesh size, which is done with the Tiedtke's mass flux scheme (TIEDTKE, 1989). CCLM_2 employs more realistic external parameter fields (e.g., topography, soil texture) which have been derived from higher-resolution observational datasets. Noteworthy are finally the different characteristic turbulent length scales (500 m for CCLM_25 against 200 m for CCLM_2), where the latter choice strongly impacts the simulated convective precipitation at 2.2 km (KOLLER, 2007).

2.2 Observational data

For the validation of CCLM_2, we consider several observational data sets. None of them is fully appropriate in the sense that they either lack spatial/temporal resolution and/or do not cover the full integration domain.

Regarding precipitation, we utilize radar observations (RAD) and rain-gauge measurements (GAUGE) both provided by MeteoSwiss. The radar observations cover Switzerland and parts of the neighboring countries (see e.g., Fig. 2). The spatial and the temporal

resolution employed here is 0.02° and 1 h, respectively. The data have been quality controlled and corrected for ground clutter, shielding, and other effects (see GERMANN et al., 2006, for more details). The GAUGE data set contains daily-accumulated precipitation records from 482 rain gauges located over Switzerland. Following the methodology of FREI and SCHÄR (1998), the data have been interpolated on a ∼0.02° grid. The effective horizontal resolution amounts to 10–15 km over flat terrain and to 15–20 km over the Alps. In addition to their daily sums, the measurements have been disaggregated into hourly values. Radar sequences are here used to distribute the daily-accumulated values over each of the 24 hours (see WÜEST et al., submitted). This secondary data set is called GAUGERAD. It is only available over Switzerland.

Even if all data sets utilize sophisticated analysis procedures, they still bear some uncertainties. Radar observations can very well capture the precipitation evolution and distribution, but the estimated rain amounts can be strongly biased (by up to a factor of two, see GERMANN et al., 2006). The rain-gauge measurements, on the other hand, suffer from a general underestimation (in mean in summer about 10 %) due to wind effects and the small-scale nature of moist convection (see FREI and SCHÄR, 1998). In addition, rain gauges are predominantly located in valleys, leading to a misrepresentation of orographic precipitation.

For the validation of temperature and relative humidity, measurements collected at the ANETZ surface stations of MeteoSwiss are used. The ANETZ network comprises 73 stations located over Switzerland, both over flat and over mountainous terrain. Due to its restricted spatial extent, we also consider the monthly temperature time series from WILLMOTT and MATSUURA (2007). The latter data set has global coverage, but its spatial resolution only amounts to 0.5°.

Finally, radiation is compared against the Baseline Surface Radiation Network (BSRN, see OHMURA et al., 1998) and against ANETZ observations. The latter only provide downward radiation, while the BSRN data set allows a validation of the different components of the radiation budget. The sparse number of the BSRN stations constitutes its major drawback. For the considered time period and integration domain, only the measurements collected at Payerne (Switzerland) come into question.

3 Results

3.1 Precipitation

Figure 2 shows total monthly precipitation for the two observational data sets RAD and GAUGE, for CCLM_2, and for its driving simulation CCLM_25. Consideration of Figs. 2a and 2c indicates that CCLM_2 is able to capture the overall precipitation distribution by reproducing most of the precipitation maxima visible in RAD (e.g., the northern Alpine slopes, the southern end of the Jura chain, the Ticino in Switzerland and its surrounding, or the French Alps). However, pronounced differences exist between simulated and observed amounts. Compared to RAD in Fig. 2a, CCLM_2 underestimates precipitation, but radar measurements bear large uncertainties (see section 2.2 and GERMANN et al., 2006). Compared to GAUGE in Fig. 2b, CCLM_2 especially overestimates the precipitation amounts over the northern Alpine slopes while too little rain falls over the eastern part of the Swiss Plateau. Overprediction of rainfalls over the windward mountain slopes is a common feature of high-resolution integrations due to the strong orographic forcing (see e.g., STEPPELER et al., 2003a; AHRENS et al., 2003; MASS et al., 2002).

With respect to CCLM_25 (see Fig. 2d), CCLM_2 yields a finer-scale and as such more realistic precipitation pattern. Interestingly and despite the use of a relatively small integration domain, CCLM_2 does not simply replicate CCLM_25. Large differences between the two integrations can for instance be found over France. In mean, CCLM_2 produces less precipitation than CCLM_25. The area-mean value amounts to 67 mm in CCLM_2 versus 72 mm in CCLM_25 (averaged over the CCLM_2 computational domain). Given the uncertainties in the recorded rain amounts (see Figs. 2a, b), it is difficult to conclusively assess the performance of CCLM_2 with regard to CCLM_25. The location of the regions with enhanced precipitation (Figs. 2a, c, d) seems nevertheless to be better captured in CCLM_2 than in CCLM_25. This might be linked to the use of a more realistic topography in CCLM_2, as many of the maxima observed in Fig. 2a are bound to orographic features.

Figure 3 displays the corresponding time series of precipitation averaged over Switzerland. CCLM_2 agrees qualitatively with RAD and GAUGERAD in the sense that CCLM_2 yields more intense rainfalls towards the beginning (5–8) and end (27–30) of July and correspondingly weaker amounts during the remaining period. Synoptically, these events can be cast into strong (5–8 and 27–30 July) and weak synoptic-scale forcing.

During the phases of strong synoptic forcing (see Fig. 3), observations and simulations show good agreement, although there is not a perfect one-to-one mapping between GAUGERAD or RAD and CCLM_2. The evolution is here better captured in CCLM_2 than in CCLM_25. For instance, the pronounced precipitation peak on July 5 is almost completely missed by CCLM_25, but qualitatively captured by CCLM_2. From 9 to 26 July 2006, the different curves in Fig. 3 generally disagree. Peak rainfall values in RAD are more than twice as high as in GAUGERAD and the latter are more than twice as high as in CCLM_2 (see especially 12–22 July). Since GAUGERAD at best underestimates precipitation, it can be concluded that CCLM_2 exhibits a systematic and pronounced tendency to underestimate

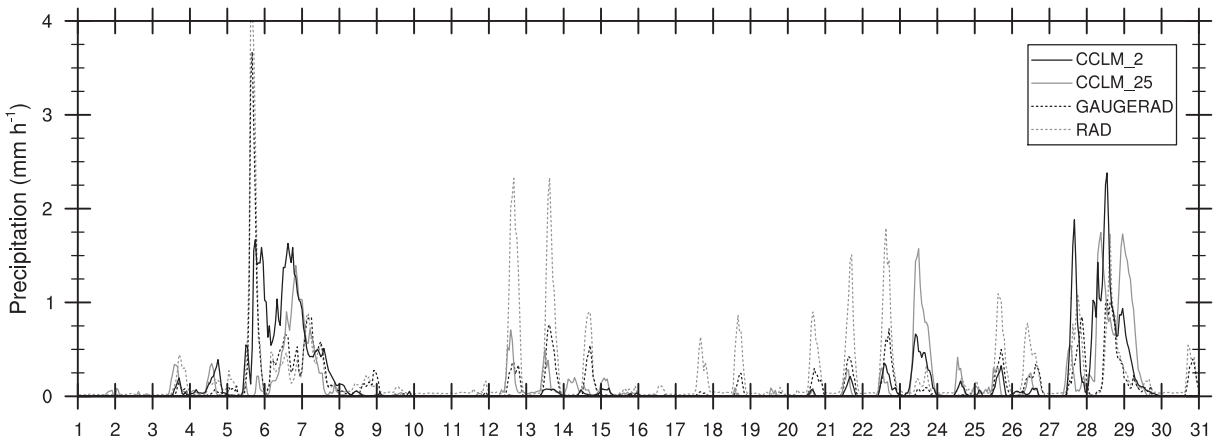

Figure 3: Time series of precipitation (mm h^{-1}) averaged over Switzerland for RAD, GAUGERAD, CCLM_25, and CCLM_2. The x-axis labels are the July days. In case of missing observations at individual grid points, the corresponding simulation values have been masked when computing the domain average.

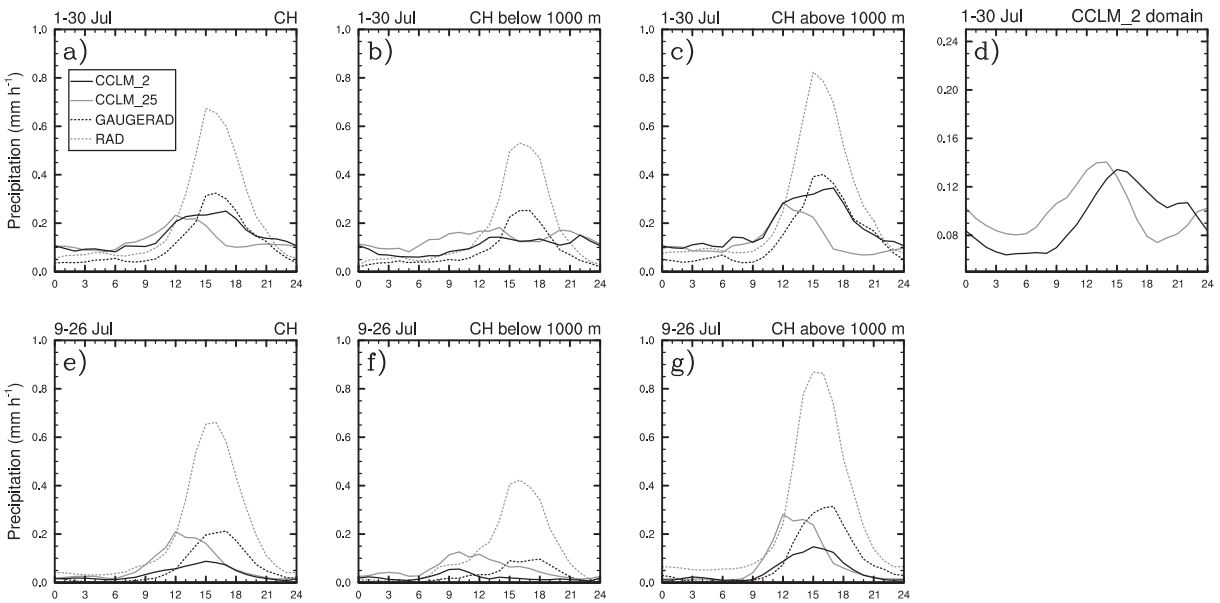

Figure 4: Diurnal cycle of precipitation (mm h^{-1}) in RAD, GAUGERAD, CCLM_25, and CCLM_2 for (a–d) 1–30 July 2006 and (e–g) 9–26 July 2006 averaged (a, e) over Switzerland (CH), (b, f) over Switzerland below 1000 m, (c, g) over Switzerland above 1000 m, and (d) over the CCLM_2 computational domain. Only nonmissing values are considered. Time in UTC.

unforced diurnal convective rainfalls. In comparison to CCLM_25 for this subperiod, the explicit treatment of convection in CCLM_2 degrades the performance on July 12–14, while CCLM_2 yields slightly more realistic rain amounts on July 22–25.

Figures 4a–c,e–g finally illustrate the diurnal cycle of precipitation averaged over Switzerland for the whole time period, for the phase of weak synoptic forcing (9–26), and for different topographic height ranges. Panel 4d contains the corresponding diurnal cycle averaged over the CCLM_2 computational domain for the whole time period. Figure 4a reveals that CCLM_2 captures the overall diurnal cycle associated with summertime convective precipitation, although some shortcomings are visible: the build-up of the convective activity stops too rapidly (by 13 UTC against 15 UTC in GAUGERAD), the nighttime and morning amounts are too large, and the diurnal precipitation range is too small. Consideration of the remaining panels of Fig. 4 further indicates that the soundness of the simulated daily convective development in CCLM_2 strongly depends upon the strength of the underlying forcing, be it of synoptic or orographic origin. Weak synoptic (see Figs. 4e–g versus Figs. 4a–c) and/or orographic (see Figs. 4b, f ver-

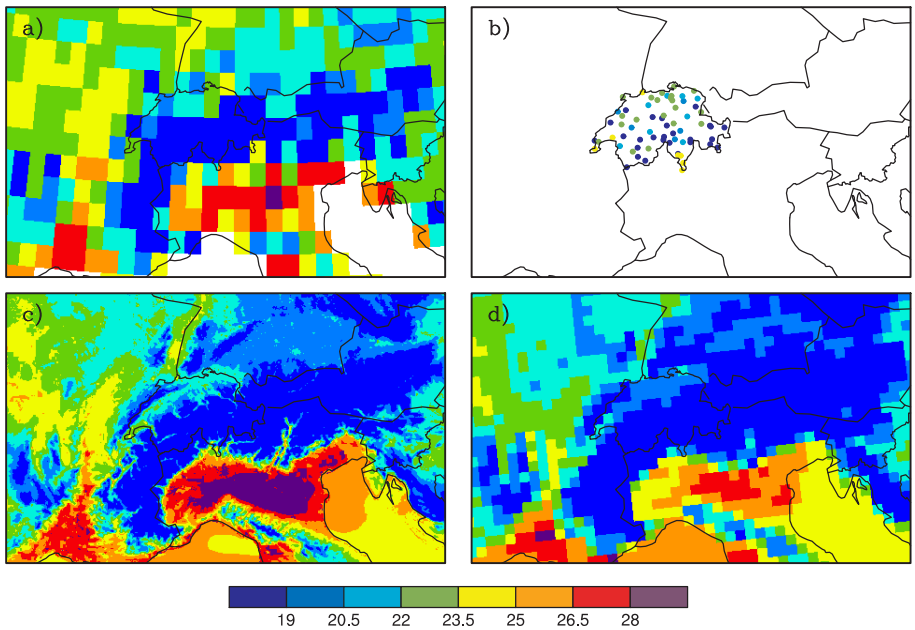

Figure 5: Monthly mean (1–30 July 2006) 2-m temperature (°C) observed in (a) WILLMOTT, (b) ANETZ, and simulated in (c) CCLM_2, and (d) CCLM_25.

sus 4c, g) forcing hampers a sound simulation of the precipitation diurnal cycle. Characteristic deficiencies in Figs. 4b–c, e–g are the underestimation of the afternoon rain amounts under weak synoptic forcing (see also Fig. 3), the combination of too strong nighttime/morning and too weak afternoon rainfalls over flat terrain, and the too early precipitation peak (or plateau) over the topography.

In comparison to CCLM_25 (see Figs. 4a–g), CCLM_2 suffers from its underestimation of daytime convective rainfalls particularly visible under weak synoptic forcing and/or over flat terrain. However, CCLM_2 mostly improves the timing of the simulated diurnal cycle. CCLM_2 exhibits a tendency towards a later onset of precipitation (e.g. of 2 h in Fig. 4d), a later maximum (2 h in Fig. 4d), and a slower decay of the convective activity. All these characteristics are in better agreement with observations and thus partly correct for some of the well-known drawbacks of the Tiedtke's mass flux scheme and of convective parameterizations in general (see e.g., DAI et al., 1999; BROCKHAUS et al., 2008).

The better timing of the convective diurnal cycle in CCLM_2 also confirms the results obtained with idealized studies using cloud-resolving and single-column models driven by prescribed large-scale forcing and surface energy fluxes (e.g., BECHTOLD et al., 2004; GUICHARD et al., 2004). As such, much of the differences visible in Figs. 3 and 4 may be seen as embedded to the use/nonuse of a convective parameterization. The fact that CCLM_2 and CCLM_25 employ distinctive topographies and simulate slightly different surface fluxes (see section 3.3) further contributes to the precipitation differences.

Hence, in terms of precipitation, the use of a cloud-resolving integration both improves and deteriorates some aspects of the simulated field. The higher resolution yields a more accurate localization of the rainfall maxima. The higher resolution can also partly correct for the too early onset and peak as well as for the too rapid decay of convective activity associated with the Tiedtke's mass flux scheme. On the other hand, the explicit treatment of deep moist convection substantially underestimates rain amounts in the afternoon, particularly in regimes with weak synoptic forcing and/or over flat terrain (see also section 4).

3.2 Temperature and relative humidity

Figure 5 displays maps of monthly mean temperature for WILLMOTT, ANETZ, CCLM_2, and CCLM_25. Note that observations and simulations employ various horizontal resolutions and orographies. Since they have not been height-corrected, differences are expected to occur over the Alpine ridge, Apennines, Massif Central, Jura, and Black Forest. We thus primarily concentrate on the remaining flatter part of the domain. Comparison of Figs. 5a, b, c indicates that CCLM_2 develops a warm bias over the Po valley and a cold bias over the northern part of our domain. Over flat terrain, the differences are generally comprised between $\pm$ 1.5 K. Consideration of Fig. 5d reveals that already the driving CCLM_25 integration exhibits a cold bias (see also JAEGER et al., 2008). The temperatures are even colder in CCLM_25 than in CCLM_2 by up to 1.5 K. As a consequence, the higher resolution improves the simulated values except over the Po valley.

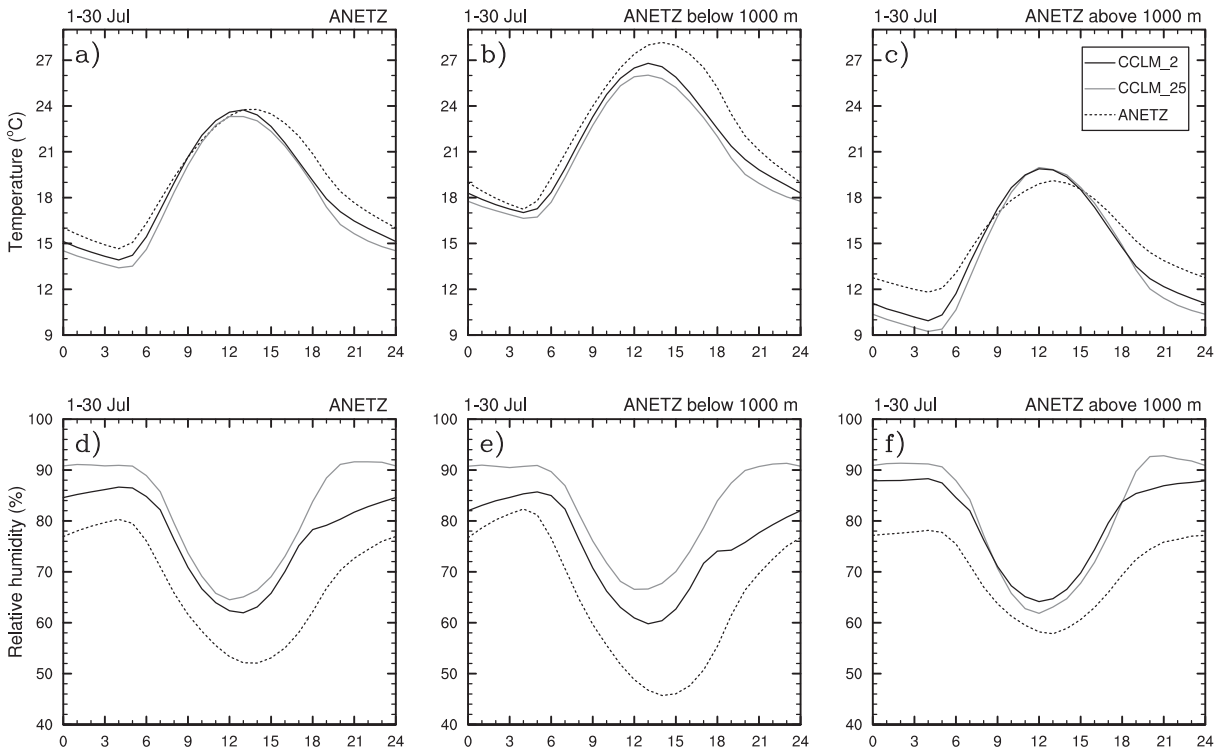

Figure 6: Monthly mean (1–30 July 2006) diurnal cycle of (a–c) 2-m temperature (°C) and (d–f) relative humidity (%) in ANETZ, CCLM_25, and CCLM_2 averaged over (a,d) all the ANETZ stations, (b, e) the stations below 1000 m, and (c, f) the stations above 1000 m. The temperature values in (a–c) have been corrected for height differences between stations and grid boxes assuming a lapse rate of 0.65 K/100 m (see text for more details). Time in UTC.

Figure 6 illustrates the monthly averaged diurnal cycle of 2-m temperature and relative humidity for three height ranges obtained with ANETZ, CCLM_2, and CCLM_25. For CCLM_25, only those grid boxes that also contain ANETZ measurements are considered. For CCLM_2, the grid box with the smallest altitudinal difference, searched in a 10-km radius around each station, is taken into account. In both cases, the 2-m temperature values have been height-corrected with a lapse rate of 0.65 K/100 m. The relative humidity is not corrected.

Figure 6a points to a slight underestimation of the temperature in CCLM_2 by 1 K and 0.4 K at 00 UTC and 14 UTC, respectively. The magnitude and sign of this bias depend upon the considered height range (see Figs. 6b, c) and time period. The daytime temperature maximum biases switch from negative (–1.5 K at 14 UTC) to positive (0.7 K at 13 UTC) between flat terrain and topography, while the nighttime temperature minimum biases are smaller over flat terrain (–0.7 K versus –1.7 K at 00 UTC, see Figs. 6b and 6c). This results in a slightly too small (too large) diurnal temperature range over flat terrain (over topography). Consideration of the subperiod 9–26 July does further increase the daytime biases to –2 K and 1 K over flat terrain and topography, respectively (not shown). Figures 6a–c finally reveal a too early maximum and afternoon cooling in CCLM_2 (by about 1 h) as compared to ANETZ. This actually yields larger temperature biases in the late afternoon than at the time of the daily peak over flat terrain. In comparison to CCLM_25, it can be concluded that CCLM_2 improves the simulated temperature diurnal cycle over Switzerland, even if both simulations are generally nearer to each other than to the observations.

Concerning the relative humidity, Figs. 6d–f reveal that CCLM_2 is too moist. Although the overall humidity evolution is approximately captured, some timing differences between ANETZ and CCLM_2 are visible. The morning reduction of the relative humidity is for instance delayed in CCLM_2 over flat terrain, while the afternoon moistening occurs ahead of time (Fig. 6e). The higher relative humidity in CCLM_2 not only follows from the generally too cold temperatures but especially from a too high absolute moisture content (not shown). Computation of the saturation deficit pinpoints to a 3-K underestimation at 14 UTC over Switzerland. Even if some of the humidity differences are large, they are generally smaller than in CCLM_25.

3.3 Radiation

Figure 7 illustrates the diurnal cycle of the different components of the surface radiation budget obtained in Payerne. This station is situated in western Switzerland near the Jura chain at an elevation of 490 m. Figure 7a

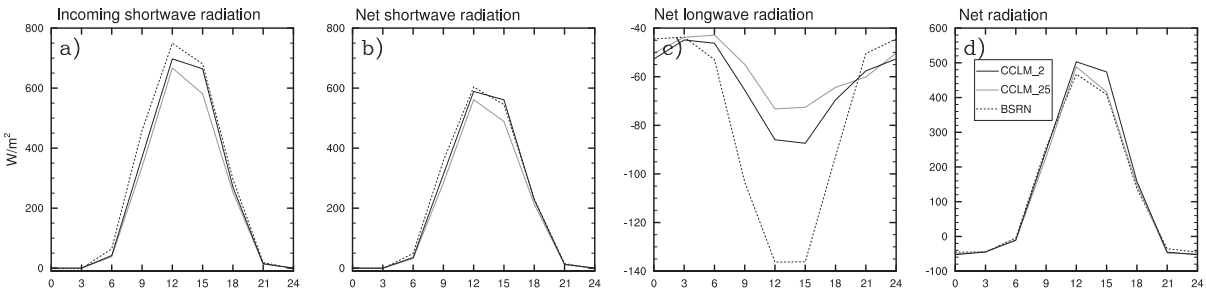

Figure 7: Monthly mean (1–30 July 2006) simulated and measured (a) shortwave incoming radiation, (b) net shortwave radiation, (c) net longwave radiation, and (d) net radiation obtained at the earth surface in Payerne (W/m^2). Time in UTC.

pinpoints to an underestimation (–52 W/m^2 at 12 UTC) of the incoming solar radiation in CCLM_2, whereas the shortwave net radiation (see Fig. 7b) is fairly well captured. This suggests a too large albedo at this grid point. The differences in longwave net radiation (see Fig. 7c) amount to 50 W/m^2 at 12 UTC. Combination of the biases in Figs. 7b and 7c results in Fig. 7d in a slightly too large net energy budget in CCLM_2. Similar considerations hold for CCLM_25 albeit with larger differences in Figs. 7a–c and for the phase of weak synoptic forcing. The magnitude of the biases in Fig. 7 should nevertheless be taken with some care, as the validation of a chaotic system at one single grid point is not unproblematic. Consideration of shortwave downward radiation measurements collected at the ANETZ stations (not shown) allows to confirm the general underestimation over flat terrain (–12 W/m^2 at 12 UTC), while a slight overestimation can be found over mountainous regions (6 W/m^2 at 12 UTC).

The obtained biases in the incoming solar radiation may follow from biases in the absorption and/or scattering by aerosols and/or clouds. Computation of clear-sky incoming shortwave radiation (not shown) reveals a good agreement between measurements and simulations at 12 UTC. This result is consistent with a previous analysis of the aerosol representation in regional climate simulations by HOHENEGGER and VIDALE (2005). Over southern Europe, they found a too large aerosol load and consequently an underestimation of solar radiation, while over Switzerland the clear-sky values coincided well with the observations in July (see their Fig. 7). Although HOHENEGGER and VIDALE (2005) used the Climate High-Resolution Model (CHRM), their results in terms of clear-sky radiation are still applicable since the two models employ the same radiation packages and aerosol distributions. It can thus be concluded that the biases in shortwave downward radiation mainly follow from biases in the cloud cover.

4 Discussion

Although the available observations only covered parts of our computational domain and were of different origin and resolution, a coherent picture of the CCLM_2 biases seems to emerge from the previous section. CCLM_2 likely overestimates the cloud cover, at least over flat terrain. The latter overprediction of clouds is consistent with the underestimated downward radiation, the too high relative humidity and the generally too cold temperature values observed in the planetary boundary layer. Given that CCLM_2 seems to overestimate the net energy budget, the previous biases also imply a wrong energy partition between sensible and latent heat fluxes and are consistent with an overestimation of the latent heat flux. These considerations especially hold over the central to northern part of our domain. Over the southern part, the lower soil moisture content may effectively limit evapotranspiration thus allowing warmer (and even too warm) temperatures, as observed in Fig. 5. This is also partly true for mountainous regions, where the lower soil moisture content and the reduced vegetation cover naturally limit the latent heat flux.

With respect to precipitation, biases in the simulated amounts are naturally expected from biases in sensible and latent heat fluxes. This is especially true for episodes with weak synoptic forcing, where the model strongly relies on the simulation of its energy and water cycles. Over the topography and/or under strong synoptic-scale forcing, the forcing indeed ensures a deep lifting of the moist unstable air. This is in agreement with our findings in section 3.1. The important role of land-surface processes for a sound simulation of the summer climate and of precipitation in particular has been highlighted in numerous studies (e.g., VIDALE et al., 2003; HAGEMANN et al., 2004; SENEVIRATNE et al., 2006; FISCHER et al., 2007). Also, several process studies have demonstrated the sensitivity of convective precipitation to the Bowen ratio by perturbing the initial soil moisture content (see e.g., SCHÄR et al., 1999; FINDELL and ELTAHIR, 2003).

The observed overestimation of the cloud cover might also impact upon the simulated precipitation amounts in a detrimental way through its feedback on the energy budget. Moreover, since clouds are overpredicted but precipitation is underestimated, CCLM_2 likely generates a wrong distribution of clouds. We tested this hypothesis by modifying the cloud di-

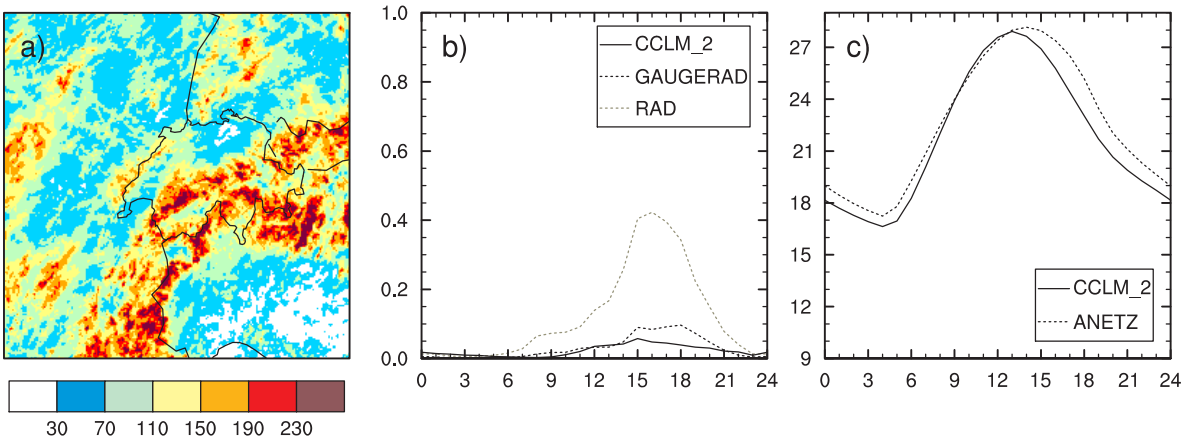

Figure 8: As (a) Fig. 2c, (b) Fig. 4f, and (c) Fig. 6b but without the consideration of subgrid-scale clouds in the CCLM_2 simulation.

agnostics, where we discarded the parameterization of subgrid-scale clouds. The simulated cloud cover thus equates to 1 or 0 only, depending on the presence/absence of cloud water or ice. This approach is partly justified since our grid spacing allows the explicit resolution of a large part of the cloud spectrum. Selected results from this experiment are shown in Fig. 8. The simulated precipitation (see Figs. 8a, b versus Figs. 2c and 4f) shows a strong sensitivity to the treatment of subgrid-scale clouds. The new integration yields a more vigorous convective activity, also over flat terrain (Fig. 8b versus Fig. 4f). The domain-mean accumulated precipitation amounts to 88 mm (compared to 67 mm in the previous simulation, see section 3.1). The new integration also simulates warmer temperatures (Fig. 8c as compared to Fig. 6b). These characteristics are generally in better agreement with the observations. Precipitation and temperature strongly benefit from corresponding increases in net radiation (+16 W/m^2 in the new simulation as compared to the previous CCLM_2 run), sensible (+7 W/m^2), and latent heat (+8 W/m^2) fluxes. In return, the fluxes might be overestimated. Comparison to the observations in Payerne indicates that the incoming solar radiation and the net radiation are overestimated by 37 W/m^2 and 97 W/m^2, respectively. These discrepancies appear large, but as stated in section 3.3, the validation of a chaotic system at one single grid point is not fully straightforward. Based on longer-term lower-resolution integrations with the CCLM covering a larger domain (JAEGER et al., 2008), we definitively believe that the obtained changes in radiation go in the proper direction. The overestimation of the incoming solar radiation is also logical in the sense that the new simulation totally lacks a representation of shallow clouds. One way to circumvent this problem would be to change the humidity threshold used in the SLINGO (1987) algorithm to assess the presence of subgrid-scale clouds. It can indeed be argued that, in line with the refinement of the grid spacing, the humidity threshold should be accordingly raised.

The previous paragraphs have uncovered some consistencies between the encountered biases. Even if it is difficult to unequivocally trace back these errors down to parameterization inaccuracies due to compensation of model errors, the land surface-soil model and/or the cloud diagnostics may be pointed at. Two further effects can be mentioned. First, the employed model mesh size of 2.2 km is too coarse to fully resolve moist convection. As shown in SKAMAROCK (2004), a grid spacing of 2.2 km corresponds to an actual horizontal resolution of about 15 km (7Δx). Hence, within our modeling setup, only deep convection can be truly resolved, implying an overall precipitation underestimation. In the same line, BRYAN et al. (2003) have for instance indicated that a grid spacing of O(100 m) is needed to properly resolve convection, although mesh sizes of O(1 km) can still provide valuable information.

Second, the CCLM_2 biases strongly recall those of CCLM_25. They are also mostly consistent with those found in JAEGER et al. (2008) for their 50-km CCLM simulation. JAEGER et al. (2008) also noted a likely overestimation of the cloud cover and errors in the energy partition between sensible and latent heat fluxes. Hence, part of the deficiencies characterizing the 2.2-km integration may be seen as imbedded to the model version and/or inherited from the coarser-resolution simulation through the forcing of the lateral boundary conditions rather than to the cloud-resolving resolution (see WARNER et al. (1997) for a discussion of the effects of the lateral boundary conditions on a limited-area model solution).

5 Conclusion

In this pilot study, the suitability of cloud-resolving resolution for climate applications has been assessed. One full month has been integrated with the CCLM on a 2.2-km grid spacing. The computational domain covers the entire Alpine ridge and contains 501 by 301 by 45

grid points. The chosen month, July 2006, was characterized by high temperatures and strong convective activity which makes it a difficult case to simulate. The boundary conditions derive from a CCLM simulation using a 25-km mesh size. The cloud-resolving resolution allows a better representation of topography and surface fields and an explicit treatment of deep moist convection. As convective parameterizations are a known source of major uncertainties and errors (e.g., MOLINARI and DUDEK, 1992; BROCKHAUS et al., 2008), cloud-resolving integrations are hoped to improve the simulated summertime precipitation distribution.

From a technical point of view, the integration of cloud-resolving simulations on climatological time scales requires an appropriate model formulation (e.g., nonhydrostatic), high-end performance computing, and generous storage capabilities. The integration has been performed on the CRAY XT-3 at the Swiss National Supercomputing Centre (CSCS) and employed 12 CPU hours on 128 dual-core nodes for one month-long simulation.

From a climatological point of view, the comparison of the simulation with observations reveals several interesting results. The cloud-resolving integration is able to capture the overall precipitation distribution and evolution. However, the nighttime amounts are overestimated, while the afternoon rainfall values are underestimated. The latter underestimation is particularly strong under weak synoptic and/or orographic forcing with values less than half as high as recorded. The temperature biases are comprised between ± 1.5 K. The negative differences dominate except over the Po valley and over mountainous regions around midday. The cloud-resolving integration also yields too high relative humidity values. Finally, for one station located over flat terrain, the validation of the radiation budget reveals an underestimation of incoming solar and outgoing longwave radiation as well as an overestimation of downward longwave radiation and of the net radiation budget at the earth surface. The biases appear generally consistent with each other and further pinpoint to an overestimation of nonprecipitating clouds and/or to a wrong energy partition between sensible and latent heat fluxes.

In comparison with its driving lower-resolution integration, the use of cloud-resolving resolution has three major advantages. First, the more realistic orographic representation allows a better localization of the precipitation maxima. Second, the cloud-resolving simulation yields warmer temperatures (by up to 1.5 K) and thus reduces the characteristic cold bias associated with the employed CCLM version (see JAEGER et al., 2008). Third and most importantly, the explicit resolution delays by 2 h (as averaged over the computational domain) the onset of convective precipitation, shifts the time of peak precipitation by a similar period, and slows down the decay of convective activity in the afternoon. This partly corrects some of the well-known biases of the Tiedtke's mass flux scheme (see BROCKHAUS et al., 2008). In return, the cloud-resolving integration strongly underestimates precipitation over flat terrain and/or during episodes with weak synoptic-scale forcing. This latter effect may be improved by modifying the treatment of subgrid-scale clouds in the model.

In general, the 2.2-km simulation is more akin to the 25-km integration than to the observations. The biases are also mostly consistent with each other. Hence, much of the deficiencies seem to be bound to the employed CCLM version and/or inherited from the coarser simulation through the lateral boundary conditions. In that respect, the cloud-resolving integration would indirectly benefit from any improvement in its driving simulation, but the higher resolution clearly possesses the additional advantage of yielding a more realistic precipitation diurnal cycle. This latter aspect is especially difficult to improve in simulations using convective parameterizations. Given the promising results obtained with July 2006, work is in progress to extend the simulations and analysis to other months and years.

Acknowledgments

The numerical simulations have been performed on the CRAY XT-3 at the Swiss National Supercomputing Centre (CSCS) in the framework of the Swiss-ALPS grant. Partial support for this study has been provided by the Swiss National Science Foundation through NCCR climate and by the European commission (ENSEMBLES project). The authors would like to thank MeteoSwiss, Daniel LEUENBERGER, Christoph FREI and Marc WÜEST for providing some of the observational data. Discussion with Eric Jäger and Chris Bretherton, technical support from Daniel Lüthi, and the reviewers' comments are acknowledged.

References

AHRENS, B., K. JASPER, J. GURTZ, 2003: On Aladin precipitation modeling and validation in an Alpine watershed. – Annales Geophysicae **21**, 627–637.

ARAKAWA, A., 2004: The cumulus parameterization problem: Past, present, and future. – J. Climate **17**, 2493–2525.

BECHTOLD, B., J.P. CHABOUREAU, A. BELJAARS, A.K. BETTS, M. KÖHLER, M. MILLER, J.L. REDELSPERGER, 2004: The simulation of the diurnal cycle of convective precipitation over land in a global model. – Quart. J. Roy. Meteor. Soc. **130**, 3119–3137.

BLOSSEY, P.N., C.S. BRETHERTON, J. CETRONE, M. KHAROUTDINOV, 2007: Cloud-resolving model simulations of kwajex: Model sensitivities and comparisons with satellite and radar observations. – J. Atmos. Sci. **64**, 1488–1508.

BROCKHAUS, P., D. LÜTHI, C. SCHÄR, 2008: Aspects of the diurnal cycle in a regional climate model. – Meteorol. Z. **17**, 433–443.

BRYAN, G.H., J.C. WYNGAARD, J.M. FRITSCH, 2003: Resolution requirements for the simulation of deep moist convection. – Mon. Wea. Rev. **131**, 2394–2416.

CHRISTENSEN, J.H., B. HEWITSON, A. BUSUIOC, A. CHEN, X. GAO, I. HELD, R. JONES, R.K. KOLLI, W.-T. KWON, R. LAPRISE, V. MAGANA RUEDA, L. MEARNS, C.G. MENENDEZ, J. RAISANEN, A. RINKE, A. SARR, P. WHETTON, 2007a: Regional Climate Projections. – In: Climate Change 2007: The Physical Science Basis. Contribution of Working Group I to the Fourth Assessment Report of the Intergovernmental Panel on Climate Change. SOLOMON, S., D. QIN, M. MANNING, Z. CHEN, M. MARQUIS, K.B. AVERYT, M. TIGNOR, H.L. MILLER (Eds.), Cambridge Univ. Press, Cambridge, United Kingdom and New York, NY, USA.

CHRISTENSEN, J.H., T.R. CARTER, M. RUMMUKAINEN, G. AMANATIDIS, 2007b: Evaluating the performance and utility of regional climate models: the prudence project. – Climatic Change **81**, 1–6.

COLLE, B.A., J.B. WOLFE, W.J. STEENBURGH, D.E. KINGSMILL, J.A.W. COX, J.C. SHAFER, 2005: High-resolution simulations and microphysical validation of an orographic precipitation event over the Wasatch Mountains during IPEX IOP3. – Mon. Wea. Rev. **133**, 2947–2971.

DAI, A.G., F. GIORGI, K.E. TRENBERTH, 1999: Observed and model-simulated diurnal cycles of precipitation over the contiguous united states. – J. Geophys. Res. **104**, 6377–6402.

DEQUE, M., D.P. ROWELL, D. LÜTHI, F. GIORGI, J.H. CHRISTENSEN, B. ROCKEL, D. JACOB, E. KJELLSTROM, M. DE CASTRO, B. VAN DEN HURK, 2007: An intercomparison of regional climate simulations for Europa: assessing uncertainties in model projections. – Climatic Change **81**, 53–70.

DOMS, G., J.FÖRSTNER, 2004: Development of a kilometer-scale NWP-System: LMK. – COSMO Newsletter **4**, 159-167, available at http://www.cosmo-model.org

FINDELL, K.L., E.A.B. ELTAHIR, 2003: Atmospheric controls on soil moisture-boundary layer interactions. Part I: Framework development. – J. Hydrometeor. **4**, 552–569.

FISCHER, E.M., S.I. SENEVIRATNE, P.L. VIDALE, D. LÜTHI, C. SCHÄR, 2007: Soil moisture-atmosphere interactions during the 2003 European summer heatwave. – J. Climate **20**, 5081–5099.

FÖRSTNER, J., G. DOMS, 2004: Runge-Kutta time integration and high-order spatial discretization of advection-A new dynamical core for the LMK. – COSMO Newsletter **4**, 168–176, available online at http://www.cosmo-model.org

FREI, C., C. SCHÄR, 1998: A precipitation climatology of the Alps from high-resolution rain-gauge observations. – Int. J. Climatol. **18**, 873–900.

FREI, C., J.H. CHRISTENSEN, M. DEQUE, D. JACOB, R.G. JONES, P.L. VIDALE, 2003: Daily precipitation statistics in regional climate models: Evaluation and intercomparison for the European Alps. – J. Geophys. Res. **108**, 4124, DOI:10.1029/2002JD002287.

GERMANN, U., G. GALLI, M. BOSCACCI, M. BOLLIGER, 2006: Radar precipitation measurement in a mountainous region. – Quart. J. Roy. Meteor. Soc. **132**, 1669–1692.

GIORGI, F., 2006: Regional climate modeling: Status and perspectives. – Journal de physique IV **139**, 101–118.

GIORGI, F., L.O. MEARNS, 1999: Introduction to special section: Regional climate modeling revisited. – J. Geophys. Res. **104**, 6335–6352.

GRABOWSKI, W.W., 2001: Coupling cloud processes with the large-scale dynamics using the cloud-resolving convection parameterization (crcp). – J. Atmos. Sci. **58**, 978–997.

GRELL, G.A., L. SCHADE, R. KNOCHE, A. PFEIFFER, J. EGGER, 2000: Nonhydrostatic climate simulations of precipitation over complex terrain. – J. Geophys. Res. **105**, 29595–29608.

GUICHARD, F.M., J.C. PETCH, J.L. REDELSPERGER, P. BECHTOLD, J.P. CHABOUREAU, S. CHEINET, W. GRABOWSKI, H. GRENIER, C.G. JONES, M. KOHLER, J.M. PIRIOU, R. TAILLEUX, M. TOMASINI, 2004: Modelling the diurnal cycle of deep precipitating convection over land with cloud-resolving models and single-column models. – Quart. J. Roy. Meteor. Soc. **130**, 3139–3172.

HAGEMANN, S., B. MACHENHAUER, R. JONES, O.B. CHRISTENSEN, M. DEQUE, D. JACOB, P. L. VIDALE, 2004: Evaluation of water and energy budgets in regional climate models applied over Europe. – Climate Dynam. **23**, 547–567.

HELMERT, J., A. WILL, M. RASCHENDORFER, B. RITTER, J.P. SCHULZ, submitted: TERRA-An extended land surface scheme for operational numerical weather prediction and regional climate applications. – Meteorol. Z. **17**.

HOHENEGGER, C., C. SCHÄR, 2007: Atmospheric predictability at synoptic versus cloud-resolving scales. – Bull. Amer. Meteor. Soc. **88**, 1783–1793.

HOHENEGGER, C., P.L. VIDALE, 2005: Sensitivity of the European climate to aerosol forcing as simulated with a regional climate model. – J. Geophys. Res. **110**, D06201, DOI:10.1029/2004JD005335.

JACOB, D., L. BARRING, O.B. CHRISTENSEN, J.H. CHRISTENSEN, M. DE CASTRO, M. DEQUE, F. GIORGI, S. HAGEMANN, G. LENDERINK, B. ROCKEL, E. SANCHEZ, C. SCHÄR, S.I. SENEVIRATNE, S. SOMOT, A. VAN ULDEN, B. VAN DEN HURK, 2007: An inter-comparison of regional climate models for Europe: model performance in present-day climate. – Climatic change **81**, 31–52.

JAEGER, E.B., I. ANDERS, D. LÜTHI, B. ROCKEL, C. SCHÄR, S.I. SENEVIRATNE, 2008: Analysis of ERA40-driven CLM simulations for Europe. – Meteorol. Z. **17**, 349–367.

JANKOV, I., W.A. GALLUS, M. SEGAL, B. SHAW, S.E. KOCH, 2005: The impact of different WRF model physical parameterizations and their interactions on warm season MCS rainfall. – Wea. Fore. **20**, 1048–1060.

KHAIROUTDINOV, M.F., D.A. RANDALL, 2001: Cloud resolving model as a cloud parameterization in the NCAR Community Climate System Model: Preliminary results. – J. Geophys. Res. **28**, 3617–3620.

KHAIROUTDINOV, M.F., D.A. RANDALL, 2003: Cloud resolving modeling of the arm summer 1997 IOP: Model formulation, results, uncertainties, and sensitivities. – J. Atmos. Sci. **60**, 607–625.

KOLLER, M., 2007: Die Rolle von numerischen Verfahren und Parametrisierungen in atmosphärischen Simulationen mit expliziter Konvektion. – Master thesis, ETH Zurich, 79 pp.

LEUNG, L.R., L.O. MEARNS, F. GIORGI, R.L. WILBY, 2003: Regional climate research – needs and opportunities. – Bull. Amer. Meteor. Soc. **84**, 89–95.

LEUNG, L.R., Y.H. KUO, J. TRIBBIA, 2006: Research needs and directions of regional climate modeling using WRF and CCSM. – Bull. Amer. Meteor. Soc. **87**, 1747–1751.

MASS, C.F., D. OVENS, K. WESTRICK, B.A. COLLE, 2002: Does increasing horizontal resolution produce more skillful forecasts? – Bull. Amer. Meteor. Soc. **83**, 407–430.

MCGREGOR, J.L., 1997: Regional climate modelling. – Meteor. Atmos. Phys. **63**, 105–117.

METEOFRANCE, 2006: Bilans climatiques annuels: 2006. – available at www.meteofrance.fr/FR/climat/clim_france.jsp

MIURA, H., M. SATOH, H. TOMITA, A.T. NODA, T. NASUNO, S. IGA, 2007: A short-duration global cloud-resolving simulation with a realistic land and sea distribution. – Geophys. Res. Lett. **34**, L02804, DOI:10.1029/2006GL027448.

MOLINARI, J., M. DUDEK, 1992: Parameterization of convective precipitation in mesoscale numerical models – a critical review. – Mon. Wea. Rev. **120**, 326–344.

OHMURA, A., E.G. DUTTON, B. FORGAN, C. FROHLICH, H. GILGEN, H. HEGNER, A. HEIMO, G. KONIG-LANGLO, B. MCARTHUR, G. MULLER, R. PHILIPONA, R. PINKER, C.H. WHITLOCK, K. DEHNE, M. WILD, 1998: Baseline Surface Radiation Network (BSRN/WCRP): New precision radiometry for climate research. – Bull. Amer. Meteor. Soc. **79**, 2115–2136.

PIELKE, R.A., J. ADEGOKE, A. BELTRAN-PRZEKURAT, C.A. HIEMSTRA, J. LIN, U.S. NAIR, D. NIYOGI, T.E. NOBIS, 2007: An overview of regional land-use and land-cover impacts on rainfall. – Tellus **59**, 587–601.

RANDALL, D., M. KHAIROUTDINOV, A. ARAKAWA, W. GRABOWSKI, 2003: Breaking the cloud parameterization deadlock. – Bull. Amer. Meteor. Soc. **84**, 1547–1564.

RANDALL, D., R. A. WOOD, S. BONY, R. COLMAN, T. FICHEFET, J. FYFE, V. KATTSOV, A. PITMAN, J. SHUKLA, J. SRINIVASAN,R.J. STOUFFER, A. SUMI, K.E. TAYLOR, 2007: Climate Models and their evaluation. – In: Climate Change 2007: The Physical Science Basis. Contribution of Working Group I to the Fourth Assessment Report of the Intergovernmental Panel on Climate Change, SOLOMON, S., D. QIN, M. MANNING, Z. CHEN, M. MARQUIS, K.B. AVERYT, M. TIGNOR, H.L. MILLER (Eds.), Cambridge Univ. Press, Cambridge, United Kingdom and New York, NY, USA.

RASCHENDORFER, M., 2001: The new turbulence parameterization of LM. – COSMO Newsletter **1**, 90–98, available online at http://www.cosmo-model.org

REINHARDT, T., A. SEIFERT, 2006: A three-category ice scheme for LMK. – COSMO Newsletter **6**, 115–120, available online at http://www.cosmo-model.org

RICHARD, E., A. BUZZI, G. ZÄNGL, 2007: Quantitative precipitation forecasting in the Alps: The advances achieved by the Mesoscale Alpine Programme. – Quart. J. Roy. Meteor. Soc. **133**, 831–846.

Ritter, B., J.F. Geleyn, 1992: A comprehensive radiation scheme for numerical weather prediction models with potential applications in climate simulations. – Mon. Wea. Rev. **120**, 303–325.

SCHÄR, C., D. LÜTHI, U. BEYERLE, E. HEISE, 1999: The soil-precipitation feedback: A process study with a regional climate model. – J. Climate **12**, 722–741.

SCHÄR, C., P.L. VIDALE, D. LÜTHI, C. FREI, C. HABERLI, M.A. LINIGER, C. APPENZELLER, 2004: The role of increasing temperature variability in European summer heatwaves. – Nature **427**, 332–336.

SENEVIRATNE, S.I, D. LÜTHI, M. LITSCHI, C. SCHÄR, 2006: Land-atmosphere coupling and climate change in Europe. – Nature **443**, 205–209.

SKAMAROCK, W. C., 2004: Evaluating mesoscale NWP models using kinetic energy spectra. – Mon. Wea. Rev. **132**, 3019–3032.

SLINGO, J.M., 1987: The development and verification of a cloud prediction scheme for the ECMWF model. – Quart. J. Roy. Meteor. Soc. **113**, 899–927.

STEPPELER, J., G. DOMS, U. SCHATTLER, H. BITZER, A. GASSMANN, U. DAMRATH, G. GREGORIC, 2003a: Meso-gamma scale forecasts using the nonhydrostatic model LM. – Meteor. Atmos. Phys. **82**, 75–96.

STEPPELER, J., R. HESS, U. SCHÄTTLER, L. BONAVENTURA, 2003b: Review of numerical methods for nonhydrostatic weather prediction models. – Meteor. Atmos. Phys. **82**, 287–301.

TIEDTKE, M., 1989: A comprehensive mass flux scheme for cumulus parameterization in large-scale models. – Mon. Wea. Rev. **117**, 1779–1800.

VIDALE, P.L., D. LÜTHI, C. FREI, S.I. SENEVIRATNE, C. SCHÄR, 2003: Predictability and uncertainty in a regional climate model. – J. Geophys. Res. **108**, 4586, DOI:10.1029/2002JD002810.

VIDALE, P. L., D. LÜTHI, R. WEGMANN, C. SCHÄR, 2007: European summer climate variability in a heterogeneous multi-model ensemble. – Climate Change **81**, 209–232.

WANG, Y.Q., L.R. LEUNG, J.L. MCGREGOR, D.K. LEE, W.C. WANG, Y.H. DING, F. KIMURA, 2004: Regional climate modeling: Progress, challenges, and prospects. – J. Meteor. Japan **82**, 1599–1628.

WARNER, T.T., R.A. PETERSON, R.E. TREADON, 1997: A tutorial on lateral boundary conditions as a basic and potentially serious limitation to regional numerical weather prediction. – Bull. Amer. Meteor. Soc. **78**, 2599–2617.

WILL A., M. BALDAUF, B. ROCKEL, A. SEIFERT, submitted: Physics and dynamics of the CLM. – Meteorol. Z.

WILLMOTT, C.J., K. MATSUURA, 2007: Terrestrial air temperature: 1900–2006 gridded monthly time series. – available at http://climate.geog.udel.edu/ climate

WÜEST, M., A. ALTENHOFF, C. FREI, M. HAGEN, M. LITSCHI, C. SCHÄR, submitted: A gridded hourly precipitation data set for Switzerland using rain-gauge analysis and radar-based disaggregation. – J. Climate.

WYANT, M.C., M. KHAIROUTDINOV, C.S. BRETHERTON, 2006: Climate sensitivity and cloud response of a gcm with a superparameterization. – Geophys. Res. Let. **33**, L06714, DOI:10.1029/2005GL025464.